



# Sunova spirulina Powder as an Effective Environmentally Friendly Corrosion Inhibitor for Mild Steel in Acid Medium

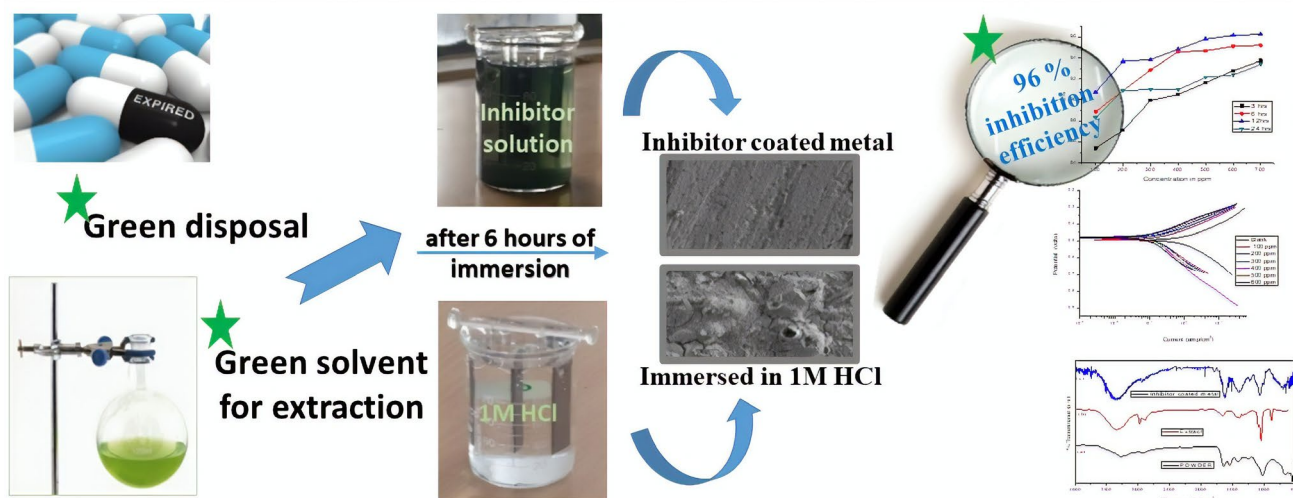
S. J. Hepziba Magie Jessima<sup>1</sup> · S. Subhashini<sup>2</sup> · James Arulraj<sup>1</sup>

Received: 4 October 2019 / Revised: 24 April 2020 / Accepted: 7 May 2020 / Published online: 17 May 2020  
© Springer Nature Switzerland AG 2020

## Abstract

*Spirulina*, blue green algae is a rich source of proteins and vitamins with excellent antioxidant properties. *Sunova spirulina* powder an effective, green corrosion inhibitor was used to evaluate its inhibition efficiency towards mild steel in 1 M HCl medium. Weight loss studies of mild steel showed an inhibition efficiency of 96% for 600 ppm concentration of inhibitor solution and 12 h of immersion period at 303 K. The percentage of inhibition efficiency increased with a step up of 10 K raise in temperature from 303 to 333 K and thereafter decreased. The results obtained were further validated by inductively coupled plasma optical emission spectrometric (ICP-OES) measurements and electrochemical techniques that included Tafel polarisation, linear polarisation and AC impedance studies. Potentiodynamic polarisation study marked the inhibitor to be a mixed type inhibiting both cathodic and anodic reactions. The adsorption studies proved that the adsorption process was spontaneous and followed Langmuir adsorption isotherm. The thermodynamic activation and adsorption parameters calculated showed that the mechanism of inhibition involved a physisorption process initially and then it slightly shifted towards chemisorption process at higher temperature. The protective layer formed on the metal surface was studied using FTIR and SEM. The complex formation between the  $Fe^{2+}$  and the active constituents of the *spirulina* extract was verified using UV visible spectra and fluorescence spectra. The effect of inhibitor concentration and temperature on corrosion rate was tested statistically using two-way analysis of variance (ANOVA) technique.

## Graphic Abstract



**Keywords** Spirulina · Green inhibitor · Mild steel · Polarisation · ICP-OES · Statistical analysis

## 1 Introduction

Mild steel or low carbon steel due to its strength, malleability, weldability and optimum mechanical properties with potentially low cost is employed in diverse applications that extend from construction, automobile parts to pipes, sheets, wires or tubes. However, metals (iron/steel) have a natural tendency to revert back to the combined state by reacting with the surrounding atmosphere resulting in rust and scale formation on its surface. So a periodic chemical cleaning of any steel equipment is necessary for its efficient functioning. The chemical plants, boilers, oil and gas pipelines make use of acid solutions for cleaning, descaling, pickling and oil well acidizing processes [1, 2]. The cleaning processes may involve several litres of acid solutions and will be repeated every 5 to 8 years. Once the scale is removed and the bare metal is exposed, the metal rapidly undergoes a classic acid corrosion leading to further dissolution of the metal [2]. This can be prevented by using corrosion inhibitor blended acid solutions.

The corrosion inhibitors vary widely from inorganic complexes, rare earth elements, organic compounds containing elements such as N, O, P and S in their heterocyclic rings, to macrocyclic compounds like porphyrin, phthalocyanin, polymers and surfactants [3]. However, synthetic inorganic and organic corrosion inhibitors are found to cause environmental pollution and hence researchers are looking for green inhibitors [4]. A vast majority of plant extracts from different parts of the world are reported to possess excellent anticorrosive properties [5]. Green inhibitors are nontoxic, easily available, and economically viable and some of them are commercially used as alternatives for the chemical inhibitors [6]. The biofilm formed by the beneficial bacterial microorganism is also utilised as one of the novel corrosion control strategies [7]. Microalgae, an inhabitant of fresh water and marine system are diverse group of organisms with potential physiological and biochemical characteristics [8]. It is referred to as the green gold of the future as it comprises large variety of unexplored group of organisms whose utility is virtually untapped [9]. *Spirulina platensis*, a blue green algae is reported to be an excellent source of proteins [10], fatty acids [11], photosynthetic pigments [12], vitamins and phenolics [13] and showed high antioxidant properties [14]. It is commercially produced so as to be used as a popular food supplement. *Spirulina* is also projected as living cell factory for the biofuel production and is widely used in food, aquaculture and pharmaceutical industries [8]. Rajendran et al. have studied the corrosion inhibition efficiency of *spirulina* for mild steel and mild steel coated zinc in artificial saliva [15]. Sribharathy and Susai Rajendran have reported the corrosion inhibition efficiency

of an aqueous extract of spirulina and sodium metavanadate solution [16]. Kamal and Sethuraman have studied the corrosion inhibition efficiency of *Spirulina platensis* powder extracted from absolute ethanol for mild steel at different temperatures in both 1 M hydrochloric acid and 1 M sulphuric acid [17]. This investigation has brought to light another important application of this microalga. The alcoholic extract of the *Spirulina platensis* with 500 ppm concentration showed inhibition efficiency of 76% for mild steel by impedance studies. Khanari et al. have reviewed the effectiveness of beta carotene in mitigation of corrosion of aluminium alloy [18]. Badawy et al. have explained the corrosion inhibition behaviour of beta carotene obtained from algal secretion. The inhibitor solution with 50 ppm concentration when tested for Cu–Al–Ni alloys in sulphide polluted chloride solutions showed 95% inhibition efficiency [19].

The present study was carried out using the acid extract of commercially available *Sunova Spirulina* (SS) capsules to explore its enhanced corrosion inhibition efficiency. The composition of SS capsule as claimed by the company in 100 g of the powder is 60 g of protein, 5 µg of vitamin B12, < 200 mg of beta carotene and slightly higher than 30 mg of iron [20]. The corrosion study was carried out using weight loss, electrochemical and spectrophotometric methods. The surface morphology was studied using SEM. The inhibitor film formed on the metal surface was characterised using IR, UV–Vis spectrophotometer and spectrofluorophotometer.

## 2 Experimental

### 2.1 Preparation of the Inhibitor Solution

1 g of the *Sunova Spirulina* (SS) powder was refluxed with 100 mL of 1 M hydrochloric acid at 353 K for 3 h and was kept overnight. The clear, supernatant liquid was then filtered and the filtrate was made up to 500 mL in a standard flask using 1 M hydrochloric acid. This was used as the stock solution for the corrosion inhibition efficiency study for mild steel.

### 2.2 Preparation of the Mild Steel Specimen

The mild steel coupons used for the present study had the following percentage composition: Fe-99.62, Mn-0.184, W-0.042, Al-0.032, Cu-0.021, C-0.017, P-0.013, Ni-0.010, Cr-0.010, Mo-0.008, S-0.008, V-0.008, Si-0.007, Nb-0.006, Pb-0.005, N-0.005, Ti-0.004. The specimen was cut into 5 × 1 × 0.2 cm dimension, mechanically polished and the

surface abraded using fine grade emery sheets. The polished metal was degreased using acetone, dried and placed in a desiccator.

### 2.3 Weight Loss Study

The weight loss studies were carried out as per ASTM G31 procedure. Accurately weighed metal coupons were immersed in 100 mL beakers containing 1 M hydrochloric acid with and without the inhibitor for a stipulated period. The immersion time was varied from 3, 6, 12 and 24 h. The experiment was repeated by varying the temperature from 303 to 343 K for an immersion period of 30 min. After each study, the coupon was again weighed accurately to find the weight loss. The experiments were performed in naturally aerated conditions and no stirring was employed. The following Eqs. (1, 2, 3) were used to calculate the inhibition efficiency, surface coverage and corrosion rate of the inhibitor.

$$\text{Inhibition Efficiency \%} = \left( \frac{W_0 - W_i}{W_0} \right) \times 100 \quad (1)$$

$$\text{Surface coverage } \theta = \left( \frac{W_0 - W_i}{W_0} \right) \quad (2)$$

$$\text{Corrosion rate (mpy)} = \frac{3.45 \times 10^6 \times \Delta W}{\rho A t} \quad (3)$$

where  $W_0$  and  $W_i$  represent the weight loss in grams for blank and inhibitor solution, respectively.  $\rho$  is the density of mild steel in  $\text{g/cm}^3$ ,  $A$  is the area of the coupon in  $\text{cm}^2$  and  $t$  is the time of immersion in hours.

### 2.4 Electrochemical Studies

CH Electrochemical workstation CHI608E model was used for the electrochemical studies namely AC impedance, LPR measurements and Tafel polarisation. The instrument makes use of three electrode cell assembly constituting platinum counter electrode, saturated calomel reference electrode and mild steel working electrode with a geometric area of  $1 \text{ cm}^2$ . The measurements were carried out after a steady state open circuit potential was established. Impedance studies were performed by applying a frequency range of 100 kHz to 1 Hz with AC signal amplitude perturbation of 0.005 V. Polarisation curves were obtained by changing the potential from  $-0.2 \text{ V}$  cathodically to  $+0.2 \text{ V}$  anodically with respect to open circuit potential and at a scan rate of  $10 \text{ mV/sec}$ .

## 2.5 Spectrophotometric Studies

### 2.5.1 ICP Optical Emission Spectra

The instrument ICP-OES spectrometer, Perkin Elmer Optima 7000 model was employed to estimate the iron content present in the blank and the inhibitor solutions obtained after the 12 h of immersion study. The inhibition efficiency obtained by weight loss studies can be further validated by this method [21]. The sample solutions enter the capillary tube of the instrument through suction. After a waiting period of 15 s the sample solutions were analysed using certified reference material for iron. The iron content in the diluted sample solutions were measured at a wavelength of 238.204 nm. From the iron content the inhibition efficiency (IE) was calculated from the Eq. (4)

$$\text{IE\%} = \left[ \left( \frac{C_0 - C}{C_0} \right) \right] \times 100 \quad (4)$$

where  $C_0$  (mg/litre) and  $C$  (mg/litre) are the concentrations of the iron present in the blank and the inhibitor solutions, respectively.

### 2.5.2 FTIR Spectra

Fourier transform infrared spectrophotometer Shimadzu IR affinity1S model was used to characterise the *Sunova Spirulina* powder, its acid extract and the inhibitor coated metal. The protective layer coated on the mild steel specimen after 6 h of immersion in the solution containing 600 ppm of the inhibitor was used for the analysis. The IR spectra were recorded from  $4000$  to  $500 \text{ cm}^{-1}$  with a resolution of  $4 \text{ cm}^{-1}$ .

### 2.5.3 UV-Vis and Fluorescence Spectra

UV spectrophotometer Shimadzu UV-1800 model and spectrofluorophotometer Shimadzu RF- 5301P model were used to record the UV-Vis absorbance and fluorescence spectra, respectively. The solutions obtained after the immersion of mild steel in 1 M HCl for 6 h with and without the inhibitor (600 ppm) were used for the studies. UV-Vis spectra were recorded from 200 to 800 nm and for fluorescence spectra the emission intensities were recorded from 300 to 800 nm.

## 2.6 Surface Analysis Studies

Field emission scanning electron microscope Carl Zeiss Sigma V model was employed for the surface analysis

study of the polished metal, inhibited and uninhibited metal. Sputtering was done using gold for 120 s at 10 mA.

### 3 Results and Discussion

#### 3.1 Effect of Inhibitor Concentrations and Immersion Periods

The inhibition efficiency of corrosion inhibitors are extensively evaluated by the weight loss technique [18]. The hetero atoms present in the active constituents of the inhibitor act as adsorption centres leading to the formation of a protective film on the metal surface. This film acts as a barrier between the metal and the aggressive medium thus inhibiting the corrosion [22]. The extent of protection increases with the inhibitor concentration as revealed by the decrease in the weight loss of the mild steel specimen [23]. Table 1 shows the performance of the acid extract of the *Sunova spirulina* of varying concentrations from 100 to 600 ppm for different immersion periods at 303 K. It was found that the inhibition efficiency reached a maximum of 96.32% for 600 ppm and 12 h of immersion time. The increased adsorption of the active molecules on the metal surface results in an enhanced surface coverage of the metal [24, 25]. The inhibitor efficiency was found to increase with the increase in immersion period up to 12 h and thereafter it decreases slightly. The decrease may be attributed to the collapse of the protective film due to its thickness exposing the metal to the acid solution. Figure 1 shows the variation of the corrosion rate with concentration of the inhibitor at different immersion periods. The corrosion rate increases with increase in the immersion period both in the absence and presence of the corrosion inhibitor. However, for a particular immersion period the inhibitor concentration shows a significant role in reducing the corrosion rate.

**Table 1** Trend in IE% with concentration of SS extract in 1 M HCl for mild steel at different immersion periods at 303 K

Conc. in ppm	Inhibition efficiency %			
	3 h	6 h	12 h	24 h
100	86.22 (1.5)	89.27 (0.4)	90.25 (0.4)	88.36 (0.1)
200	88.31 (1.8)	90.67 (0.2)	93.72 (0.1)	90.98 (0.1)
300	90.29 (0.4)	92.35 (0.5)	93.90 (0.1)	91.02 (0.0)
400	92.17 (2.1)	94.20 (0.4)	94.73 (0.1)	90.89 (0.1)
500	92.67 (1.4)	94.97 (0.3)	95.67 (0.1)	92.29 (0.1)
600	93.16 (0.7)	95.11 (0.0)	96.32 (0.2)	92.43 (0.1)

The standard deviation values are given in parentheses

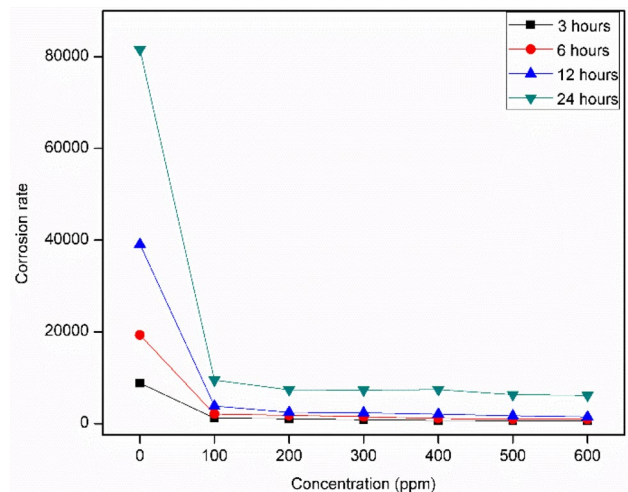


**Fig. 1** Variation of corrosion rate of mild steel with concentration of SS extract in 1 M HCl at different immersion periods

#### 3.2 Effect of Temperature

The nature of adsorption of the inhibitor molecules on the surface of the metal can be studied by monitoring the inhibition efficiency of the inhibitor at different temperatures. Table 2 shows an increase in the trend of IE % of SS extract of same concentration with a step up of 10 K raise in temperature from 303 to 333 K and half an hour of immersion period. The inhibition efficiency was found to reach a maximum of 91.30% at 333 K for 600 ppm concentration. This trend reveals that a stable protective layer was formed on the metal surface due to the chemical interaction between the active constituents of the inhibitor and the metal surface. This reveals the nature of adsorption process involved in the corrosion inhibition was chemisorption [26]. However, at 343 K there was a decrease in the inhibition efficiency % which may be due to the breaking of the adsorbed layer leading to smaller segments, exposing the surface to the aggressive medium [27]. Figure 2 reveals an increase in the corrosion rate with increase in temperature both in the absence and presence of the inhibitor. This is due to the increase in the thermal agitation of the acid medium that obviously will enhance the metal dissolution [28]. However, it can be noted that the corrosion rate decreases with the increase in SS concentration for a particular temperature due to the formation of stable protective layer on the metal surface [29].

##### 3.2.1 Thermodynamic Activation Parameters

Temperature plays an important role in influencing the rate of electrochemical corrosion. The relationship between the temperature and the corrosion rate is given by the Arrhenius Eq. (5).



**Table 2** Variation of IE % with concentration of SS extract in 1 M HCl for mild steel at different temperatures and for an immersion period of half an hour

Conc. in ppm	Inhibition efficiency %				
	303 K	313 K	323 K	333 K	343 K
100	54.32 (8.6)	76.92 (0.8)	82.26 (0.0)	86.14 (0.0)	82.38 (0.1)
200	55.56 (4.9)	79.84 (1.1)	84.72 (0.3)	86.78 (0.9)	84.10 (0.6)
300	65.43 (0.0)	80.37 (1.9)	87.04 (0.4)	89.52 (0.1)	87.10 (0.1)
400	70.37 (2.5)	83.82 (1.9)	88.81 (0.8)	89.44 (0.1)	88.88 (0.3)
500	71.60 (3.7)	84.62 (3.2)	89.09 (0.8)	90.20 (0.1)	88.73 (0)
600	87.65 (4.9)	89.92 (0.5)	90.31 (0.1)	91.30 (0.2)	88.98 (0.1)

The standard deviation values are given in parentheses

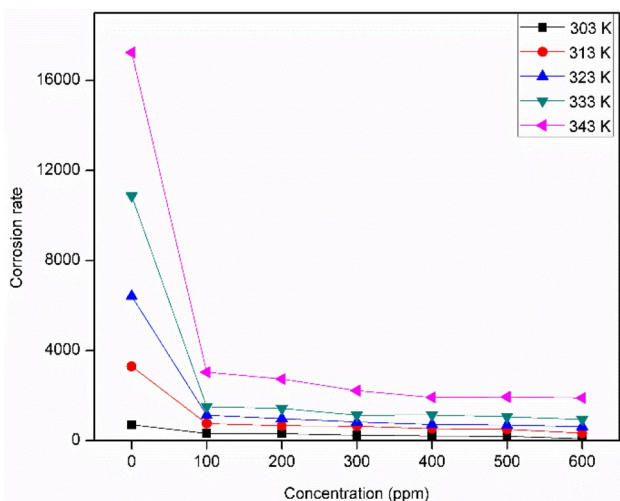


**Fig. 2** Variation of mild steel corrosion rate with temperature for different concentrations of the SS extract in 1 M HCl

$$\log CR = \frac{-E_a}{2.303RT} + \log A \tag{5}$$

where *CR* is the corrosion rate, *E<sub>a</sub>*, the apparent activation energy, *A*, the Arrhenius pre-exponential factor, *R*, the molar gas constant and *T*, the absolute temperature. The transition state Eq. (6) is used to calculate enthalpy of activation ( $\Delta H^*$ ) and entropy of activation ( $\Delta S^*$ ) for the corrosion reaction.

$$\log \frac{CR}{T} = \frac{R}{Nh} \exp \frac{\Delta S^*}{R} \exp \frac{-\Delta H^*}{RT} \tag{6}$$

where *N* is the Avagadro number and ‘*h*’ is the Planck’s constant. The thermodynamic activation parameters *E<sub>a</sub>*, *A*,  $\Delta H^*$  and  $\Delta S^*$  listed in Table 3 were obtained from the linear plots of  $\log CR$  versus  $1/T$  and  $\log (CR/T)$  versus  $1/T$ . The *E<sub>a</sub>* value for mild steel in 1 M HCl was found to be 66.33 kJ/mole which agrees well with the literature values 50–100 kJ/mole [30]. The lower values of *E<sub>a</sub>* for the inhibitor solutions than that of the blank supports the formation of chemisorbed layer of the inhibitor on the surface of the mild steel [31]. According to Eq. (5) the mild steel corrosion can be influenced by Arrhenius pre-exponential factor *A* and apparent activation energy *E<sub>a</sub>*. Greater variation of *A* with the inhibitor concentration compared to *E<sub>a</sub>* indicates that *A* may be the dominant factor in influencing the corrosion rate [32]. The lower values of  $\Delta H^*$  than that of *E<sub>a</sub>* reveals that a gaseous reaction namely the hydrogen evolution reaction was involved in the corrosion process, correlated to reduction in total reaction volume [33]. The difference between *E<sub>a</sub>* and  $\Delta H^*$  values is 2.68 kJ/mole that signifies unimolecular reaction in the corrosion process [34, 35]. The positive sign of the enthalpy of activation reveals that the metal dissolution process was endothermic in presence of the inhibitor. The sign of the  $\Delta S^*$  values changed when moving from blank to the inhibitor solution. This is attributed to the non-spontaneity of the metal dissolution process in presence of the inhibitor. The negative sign of  $\Delta S^*$  reflects orderly adsorption

**Table 3** Thermodynamic and activation parameters of the corrosion process on mild steel in 1 M HCl

Conc in ppm	<i>E<sub>a</sub></i> (kJ mole <sup>-1</sup> )	<i>A</i> (kg m <sup>-2</sup> s <sup>-1</sup> )	$\Delta H^*$ (kJ mole <sup>-1</sup> )	$\Delta S^*$ (J mol/K)	<i>E<sub>a</sub></i> - $\Delta H = RT$
Blank	66.33	$2.72 \times 10^{14}$	63.65	22.46	2.68
100	45.00	$2.04 \times 10^{10}$	42.32	- 56.51	2.68
200	44.14	$1.36 \times 10^{10}$	41.46	- 59.91	2.68
300	43.98	$1.05 \times 10^{10}$	41.30	- 62.05	2.68
400	45.08	$1.42 \times 10^{10}$	42.41	- 59.53	2.68
500	46.04	$1.95 \times 10^{10}$	43.36	- 56.90	2.68
600	64.14	$1.22 \times 10^{13}$	61.46	- 3.37	2.68

of the inhibitor molecules on the metal surface which was initially moving freely in the bulk of the solution [32].

### 3.2.2 Adsorption Isotherm

The effectiveness of the inhibitor in corrosion mitigation of mild steel in 1 M HCl solution was investigated by the use of adsorption isotherms as it correlates the surface coverage with the concentration of the inhibitor. The adsorption isotherms namely Langmuir, Temkin, Freundlich, El-Awady and Florry-Huggins isotherms were attempted. Langmuir isotherm showed a best fit as was determined by the regression values  $R^2$ . The modified Langmuir isotherm equation is

$$C/\theta = 1/K_{\text{ads}} + C \quad (7)$$

where  $C$  is inhibitor concentration,  $K_{\text{ads}}$  is adsorption equilibrium constant, and  $\theta$  is the degree of surface coverage of the inhibitor. Figure 3 shows the modified Langmuir plot of  $C/\theta$  versus  $C$  which is nearly linear and the slope was found to vary from 1.03 to 1.10 between the temperature 303 K and 343 K. This suggests the monolayer adsorption of the main constituents of SS on the mild steel surface and there is no interaction between them [36]. These observations point out that the inhibitor which was physisorbed at lower temperatures gets firmly held on the surface of the metal by chemisorption with the raise in temperature [32]. The intercept of the modified Langmuir plot is equal to  $1/K_{\text{ads}}$  and is related to the standard Gibbs free energy by the Eq. (8).

$$K_{\text{ads}} = \frac{1}{55.5} \exp\left(\frac{-\Delta G_{\text{ads}}^0}{RT}\right) \quad (8)$$

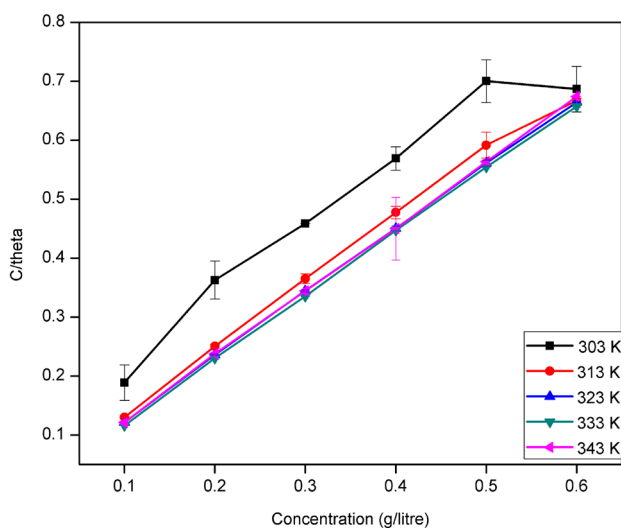


**Fig. 3** Modified Langmuir plot for mild steel in 1 M HCl in presence of SS extract

**Table 4** Adsorption parameters for the corrosion process on mild steel in 1 M HCl

Temp. (K)	$K_{\text{ads}}$	$\Delta G_{\text{ads}}^0$ (kJ mol <sup>-1</sup> )	Slope	$R^2$
303	7.75	-15.28	1.03	0.93
313	34.74	-19.69	1.09	0.99
323	64.32	-21.97	1.08	0.99
333	97.10	-23.08	1.08	0.99
343	79.37	-23.93	1.10	0.99

where  $R$  is molar gas constant, 55.5 is molar concentration of water molecules at electrode and electrolyte interface during the adsorption process and  $T$  is absolute temperature. Table 4 shows the values of  $K_{\text{ads}}$  and  $\Delta G_{\text{ads}}^0$ . High values of  $K_{\text{ads}}$  with increase in temperature indicates the formation of strong and stable adsorbed layer and consequently higher inhibition efficiency [36, 37]. The value of  $\Delta G_{\text{ads}}^0$  up to  $-20$  kJ mol<sup>-1</sup> indicates physical adsorption while a value more than  $-40$  kJ mol<sup>-1</sup> corresponds to chemisorption [38]. The calculated values of  $\Delta G_{\text{ads}}^0$  for different temperatures vary from  $-15.28$  to  $-23.93$  kJ mol<sup>-1</sup>. This shows that the adsorption process involves physisorption which slightly shifted towards chemisorption at higher temperatures. The negative value of  $\Delta G_{\text{ads}}^0$  supports the spontaneity of the adsorption process. Based on Van't Hoff Eq. (9),  $\Delta H_{\text{ads}}^0$  was calculated and found to be  $-50.02$  kJ/mole.

$$\ln K = \frac{-\Delta H_{\text{ads}}^0}{RT} + \text{Constant} \quad (9)$$

The negative value of  $\Delta H_{\text{ads}}^0$  signifies physisorption or chemisorption process [39]. According to the literature the enthalpy value for a physisorption process is less than 41.86 kJ/mole while for chemisorption it approaches 100 kJ/mole [40]. This indicates that the electrostatic interaction between the protonated inhibitor molecules and  $\text{Cl}^-$  ions could have allowed the physisorption of the inhibitor on the surface. This may be followed by the transfer of electrons from the active constituents of the inhibitor molecules to the empty 'd' orbitals of iron [32].

### 3.2.3 Statistical Analysis

The null hypotheses stating there is no significant difference in the corrosion rate due to different inhibitor concentration levels and due to different temperatures were tested using two-way analysis of variance (ANOVA) [41]. The results are given in Table 5.

Since the F-calculated values are greater than the F table values, i.e.  $6.85 > 2.36$  and  $4.29 > 2.71$ , the null hypotheses are rejected at 5% level. The study infers that the corrosion rate is significantly different for different temperatures as

**Table 5** Two way analysis of variance (ANOVA)

Source	Degrees of freedom	Sum of squares	Mean sum of squares	F	F table
Concentration	7	201,120,021.7	28,731,431.67	6.85	$F_{7, 28} = 2.36$
Temperature	4	71,916,589.49	17,979,147.37	4.29	$F_{4, 28} = 2.71$
Error	28	117,419,210	4,193,543.215		
Total	39	390,455,821.2			

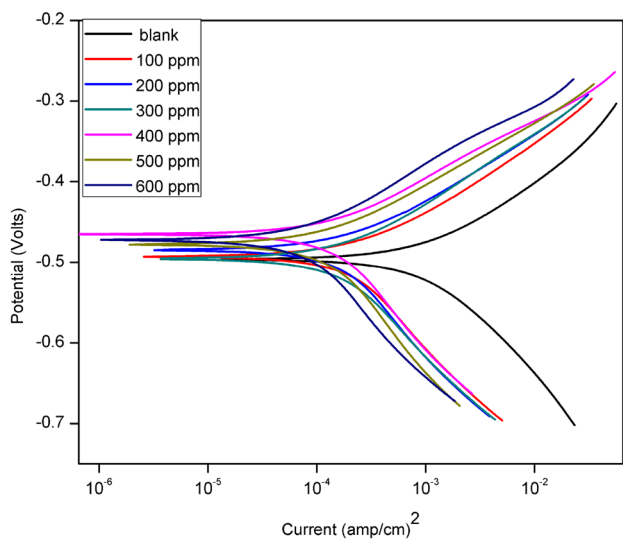


**Fig. 4** Polarisation curves obtained for mild steel in 1 M HCl solution in the presence and absence of the inhibitor

well as different inhibitor concentration levels. This means that the inhibitor concentration and temperature have significant effect on corrosion rate.

### 3.3 Electrochemical Studies

#### 3.3.1 Tafel Polarisation

Figure 4 shows the polarisation curves obtained for mild steel in 1 M HCl solution in the presence and absence of the

inhibitor. Both the cathodic and anodic curves shift towards the lower current densities on addition of the inhibitor pointing that the anodic metal dissolution and the cathodic hydrogen evolution partial reactions are efficiently inhibited by the inhibitor [42]. Table 6 provides the values of corrosion potential ( $E_{corr}$ ), corrosion current densities ( $I_{corr}$ ), cathodic tafel slope ( $\beta_c$ ) and anodic tafel slope ( $\beta_a$ ). According to the report if the difference in the  $E_{corr}$  values between the uninhibited and inhibited solution is greater than  $\pm 85$  mV then the inhibition can be labelled as anodic or cathodic type [43]. In the present study, the maximum displacement in  $E_{corr}$  values is 24.5 mV which indicates a mixed type inhibition. The inhibition efficiency calculated using  $I_{corr}$  values was found to increase with the inhibitor concentration and reached a maximum of 91.27% at 600 ppm concentration of the inhibitor. This may be attributed to both anodic and cathodic inhibition performance of the inhibitor via adsorption on the metal surface blocking the active sites [44]. Tafel slopes ( $\beta_a$ ) and ( $\beta_c$ ) were found to change with inhibitor concentration indicating mixed type of corrosion inhibition [45].

#### 3.3.2 Linear Polarisation Study

Linear polarisation measurements help to monitor the corrosion rate and the performance of the inhibitor. Table 6 shows that the linear polarisation resistance (LPR) values were higher for the inhibitor solutions than that of the blank solution. The  $LPR_{(inhibitor)}$  values were found to increase with the increase in inhibitor concentration [46]. Using Eq. (10) the inhibition efficiency (IE %) was calculated.

**Table 6** Polarisation parameters for mild steel in 1 M HCl obtained at room temperature

Conc in ppm	$E_{corr}$ (mV/SCE)	$I_{Corr}$ ( $\mu A/cm^2$ )	$\beta_c$ (mV/dec)	$\beta_a$ (mV/dec)	IE %	LPR ( $\Omega cm^2$ )	IE %
Blank	-496.9	1008	139.2	94.33		24	
100	-493.5	220.5	154.4	74.88	78.13 (3.3)	99	75.76 (3.7)
200	-486.7	182.4	164.5	75.22	81.91 (2.1)	123	80.49 (2.0)
300	-496.5	177.9	148.1	83.89	82.35 (2.4)	131	81.68 (1.8)
400	-464.9	151.5	169.72	73.56	84.97 (0.3)	147	83.67 (0.5)
500	-478.4	136.4	178.6	78.50	86.47 (1.1)	174	86.21 (1.9)
600	-472.4	88.04	176.8	76.93	91.27 (1.0)	260	90.77 (1.1)

Te standard deviation values are given in parenthesis

$$\text{inhibition Efficiency} = \frac{LPR_{(\text{inhibitor})} - LPR_{(\text{blank})}}{LPR_{(\text{inhibitor})}} \times 100 \quad (10)$$

The results were in agreement with the values obtained from weight loss studies.

### 3.3.3 Electrochemical Impedance Study

Impedance measurements give the characteristics and the kinetics of the in situ electrochemical reactions occurring at the metal/acid interface in the presence and in the absence of the corrosion inhibitor. Figure 5 shows a: Nyquist plot, b and c: Phase angle and Bode plots drawn using the results obtained from the electrochemical impedance measurements. A single capacitive loop in the Nyquist and only one time constant/ single relaxation process in phase angle plot reveals that the formation of the electrical double layer at the metal solution interface and corrosion of mild steel are controlled by the single charge transfer process [47]. The corrosion mechanism remains unchanged in the absence and presence of the inhibitor as revealed by the similar capacitive loop appearance. However, the diameter of the capacitive loop is found to increase with the increase in the inhibitor concentration. This can be correlated due to the increased efficacy of the inhibitor to be adsorbed on the metal solution interface forming a protective film and mitigate corrosion [48]. Further evidence comes from the Bodes plot which shows an increase in the absolute impedance value at lower frequencies with increase in the inhibitor concentration [49]. The inhomogeneity of the metal surface that arises from surface roughness, impurities, adsorption of the inhibitor molecules, formation of porous layers, distribution of the activity centres is reflected in the depressed semicircle of the capacitive loop in Nyquist plot [50]. The non-ideal capacitance behaviour is further supported by the phase angle plot where the increase in the phase angle with the inhibitor concentration was lower than  $-90^\circ$  [51]. This led to a necessity of replacing double layer capacitance in the Randles circuit by a constant phase element (CPE) for the best fit of the depressed semicircle. The various impedance parameters obtained by best fitting the experimental data in the equivalent circuit (Fig. 6) are given in Table 7. The best fit is revealed by the Chi-squared value [52]. The impedance of the CPE is given by the following expression [53]

$$Z_{\text{CPE}} = [Y_0(j\omega)^n] \quad (11)$$

where the  $Y_0$  refers to the magnitude of CPE,  $j$  is an imaginary number which is equal to square root of  $-1$ ,  $\omega$  is the angular frequency and  $n$  is the phase shift that corresponds to the inhomogeneity of the surface. The  $R_p$  values displayed in Table 7 denotes the polarisation resistance which constitutes charge transfer resistance, inhibitor film resistance,

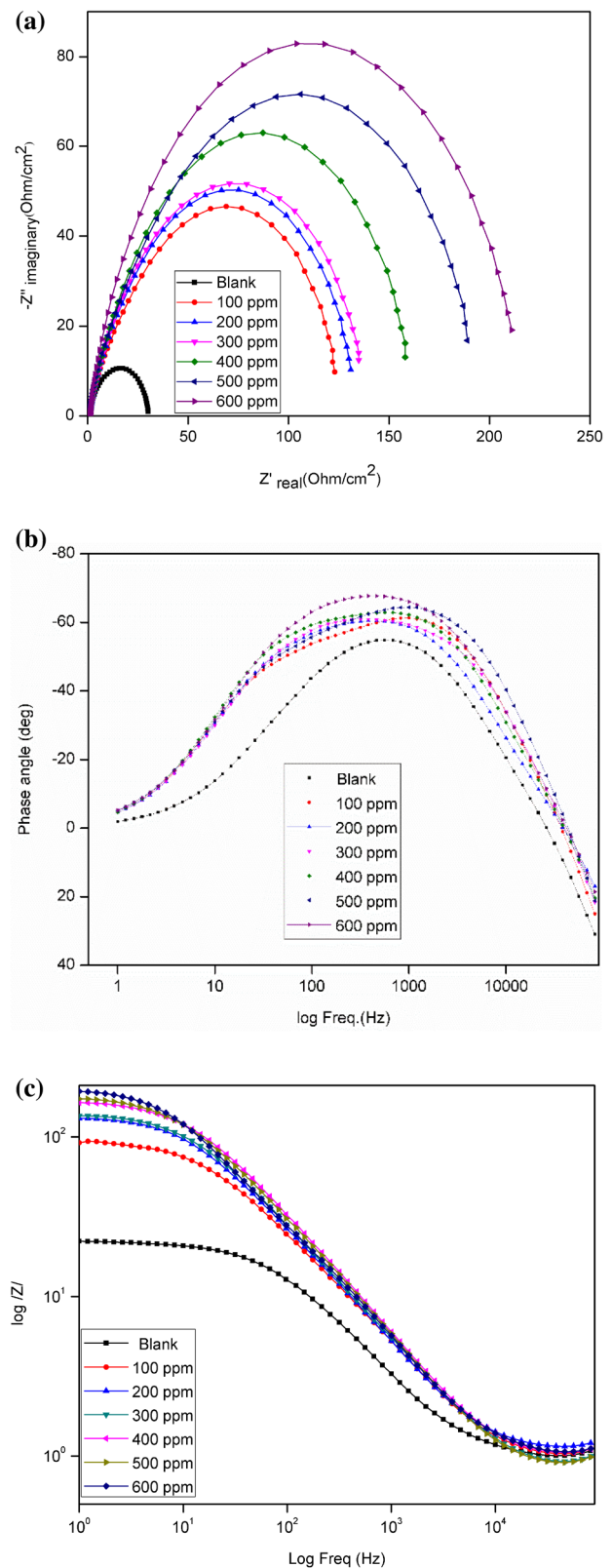


**Fig. 5** **a** Nyquist Plot obtained for mild steel in 1 M HCl both in absence and presence of SS extract at 303 K. **b** Phase angle plot for mild steel in 1 M HCl in absence and presence of the SS extract. **c** Bode Plot for mild steel in 1 M HCl in the absence and presence of the SS extract



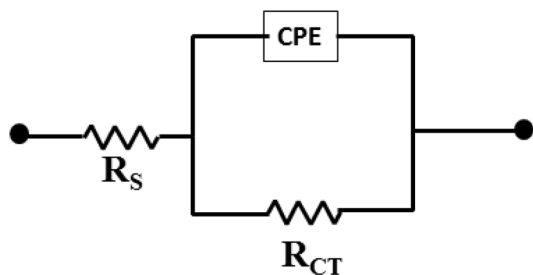


**Fig. 6** Equivalent circuit for the EIS data obtained for mild steel in 1 M HCl

diffused layer resistance and resistance of all accumulated species [54]. The interfacial double layer capacitance ( $C_{dl}$ ) values was calculated using the following relationship [42]

$$C_{dl} = (Y_0 \times R_p^{1-n})^{1/n}$$

The  $R_p$  values is found to increase while the  $C_{dl}$  values decrease with increase in concentration as shown in Table 7. This can be corroborated to the retardation of the charge transfer process due to the adsorption of the inhibitor at the metal solution interface [55].

**3.3.4 ICP- OES Measurements**

Table 8 shows the iron content of the blank and the inhibited solutions obtained after the weight loss studies using inductively coupled plasma (ICP) optical emission spectrometry (OES). The decrease in the amount of iron with the increase in the concentration of the inhibitor supports the effectiveness of the inhibitor in preventing the dissolution of iron into the solution. This may be due to the adsorption of the active constituents of the inhibitor onto the metal surface [56–58]. The inhibitor efficiency calculated from the iron content using the Eq. (4) was in agreement with the results obtained by other methods.

**Table 8** Iron content obtained by ICP-OES method

Conc. in ppm	Iron content in mg/litre	IE %
Blank	1944.5	–
200	218.0	88.7
400	154.4	92.1
600	144.0	92.6
700	132.0	93.2

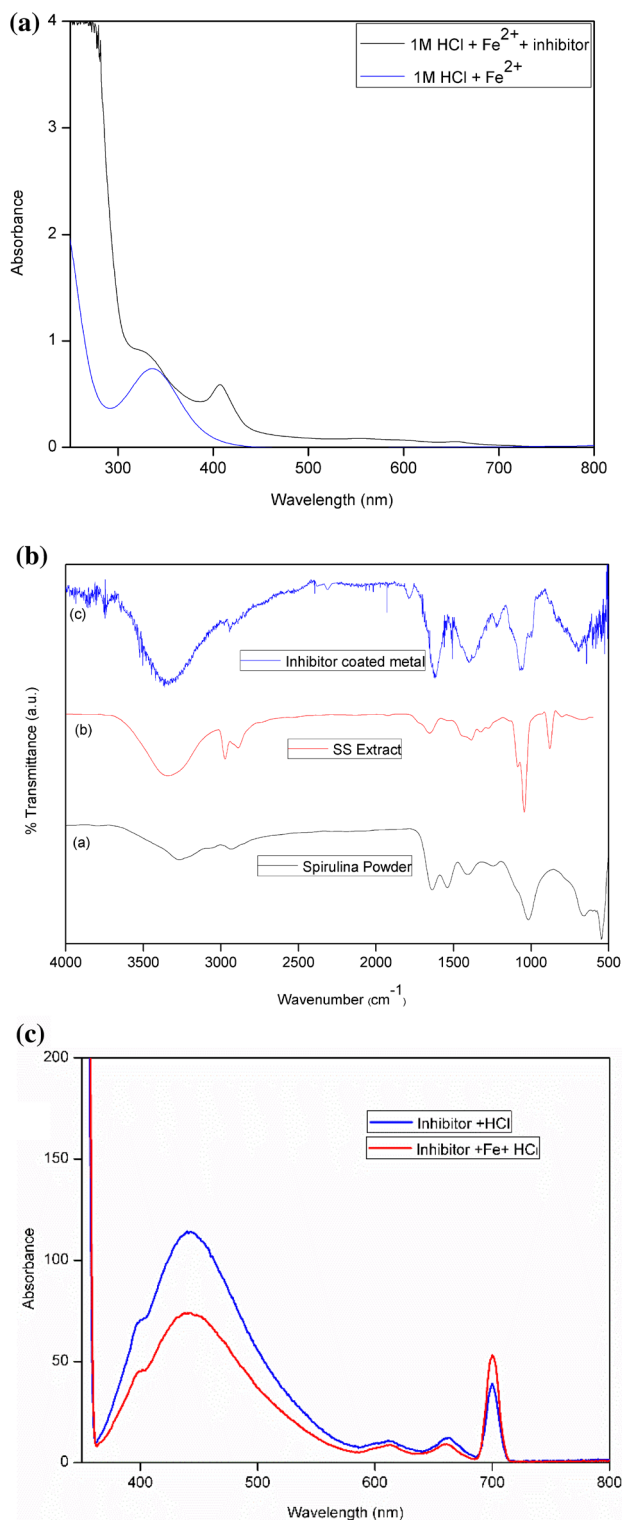
**3.4 UV Visible, FTIR and Spectrofluorometric Spectral studies**

Figure 7a shows the UV–Vis spectra of the blank solution and the inhibitor solution obtained after 6 h of immersion of the mild steel specimen. This technique is suitable for the identification of formation of the complex ion in solution. The absorption maxima was found to be shifted towards longer wavelength in the presence of the inhibitor. This indicates the complex formation between  $Fe^{2+}$  and the active constituent of the inhibitor solution [59, 60].

Figure 7b shows the FTIR spectra of the *spirulina* powder, inhibitor extract and the inhibitor coated metal. This technique is employed to ascertain that the corrosion inhibition is due to the interaction between the metal and the inhibitor molecules [61]. The S–O stretching occurring at  $1543\text{ cm}^{-1}$  has a high intensity in the powder which reduces in intensity in the acid extract probably due to protonation and this stretching shifts to a lower wave number  $1516\text{ cm}^{-1}$  in the inhibitor coated metal. This can be attributed to the binding of the R–S–O unit to the metal. This is further corroborated when we consider the S–O stretching at  $1409\text{ cm}^{-1}$  which being low in intensity in the powder and the acid extract, increases in intensity in the inhibitor coated metal. The P–O stretching occurs at  $1020\text{ cm}^{-1}$  in the powder and this shift to  $1046\text{ cm}^{-1}$  in the acid extract and then to  $1064\text{ cm}^{-1}$  in the inhibitor coated metal. This would mean that the P–O group gets protonated in the acid medium as well as in the inhibitor coated metal surface suggesting electrostatic attraction (physisorption) of the inhibitor molecules on the metal surface [62]. The IR absorption at  $1640\text{ cm}^{-1}$  in

**Table 7** Impedance parameters for mild steel in 1 M HCl in the absence and in the presence of the inhibitor

Conc. ppm	Chi-Sq $\times 10^{-2}$	$n$	$R_s$ ( $\Omega/\text{cm}^2$ )	CPE $\times 10^{-4}$	$C_{dl} \times 10^{-5}$	$R_p$ ( $\Omega/\text{cm}^2$ )	IE %
Blank	2.476	0.8346	0.8772	2.664	10.1624	29.01	
100	2.602	0.7961	0.8563	2.046	8.0036	125.2	76.82
200	1.094	0.806	1.128	1.918	7.9543	134.6	78.45
300	1.63	0.8032	0.9291	1.831	7.4613	140.0	79.28
400	1.466	0.8213	0.9765	1.570	7.0765	163.5	82.26
500	2.192	0.8122	0.9337	1.236	5.1960	190.7	83.04
600	1.178	0.8566	1.006	0.971	5.0655	211.2	86.26



**Fig. 7** **a** UV–Vis spectra of the blank and the inhibitor solutions containing  $\text{Fe}^{2+}$  ions. **b** FTIR spectra of (a) spirulina powder, (b) inhibitor extract and (c) inhibitor coated metal. **c** Fluorescence spectra of the inhibitor solution and the inhibitor solution containing  $\text{Fe}^{2+}$  ions

the powder shifts to  $1658\text{ cm}^{-1}$  in the acid extract and then to  $1622\text{ cm}^{-1}$  in the inhibitor coated metal surface matches well with the scissor bending mode of  $-\text{NH}_2$  of amide group implying the involvement of the latter in the inhibition activity [62].

Figure 7c shows the fluorescence spectra of the acid extract of the inhibitor and the inhibitor solution obtained after 6 h of immersion of the mild steel specimen. The absorption peak between 400 and 500 nm corresponds to beta carotene and that at 700 nm corresponds to chlorophyll [63]. The decrease in the intensity of absorbance peak of beta carotene obtained for the inhibitor solution containing  $\text{Fe}^{2+}$  ions shows the interaction between beta carotene and the metal ion.

### 3.5 Surface Morphology

Figure 8 shows the SEM images of (a) pure metal (b) metal in 1 M HCl and (c) metal immersed in the 600 ppm concentration of acid extract of the *Sunova spirulina* for 6 h at 298 K. On comparison, it clearly showed the corrosive attack of the acid medium on the metal surface and the corrosion rate visibly reduced on the surface of the metal in presence of the inhibitor. This is due to the uniform deposition of the inhibitor on the surface of the metal.

### 3.6 Mechanism

The experimental results clearly reveal the enhanced corrosion inhibition efficiency of the acid extract of the *Sunova spirulina* powder as compared to that of its alcoholic extract study by others.[17]. This is perhaps due to the adsorption of the active constituents of the *spirulina* extract onto the metal surface. The active constituents in the extract are the monosaccharides, amino acids and beta carotene. These constituents contain the hetero atoms in their functional groups such as  $-\text{OH}$ ,  $-\text{NH}_2$ ,  $\text{R}-\text{S}-\text{O}$ , and  $\text{P}-\text{O}$  which get protonated in acid medium. These protonated groups are then electrostatically attracted towards  $\text{Cl}^-$  adsorbed metal surface. The  $\pi$  electrons of beta carotene must be attracted towards the partially empty 'd' orbitals of  $\text{Fe}^{2+}$  resulting physisorption. This is followed by the complex formation as indicated by the spectrophotometric techniques. These interactions help in retaining the inhibitor on the metal surface even at higher temperatures.

## 4 Conclusion

The acid extract of *Sunova spirulina* powder was observed to be an effective green corrosion inhibitor for mild steel in 1 M HCl than the ones investigated with alcoholic extract of the spirulina powder by others. The inhibition efficiency increases

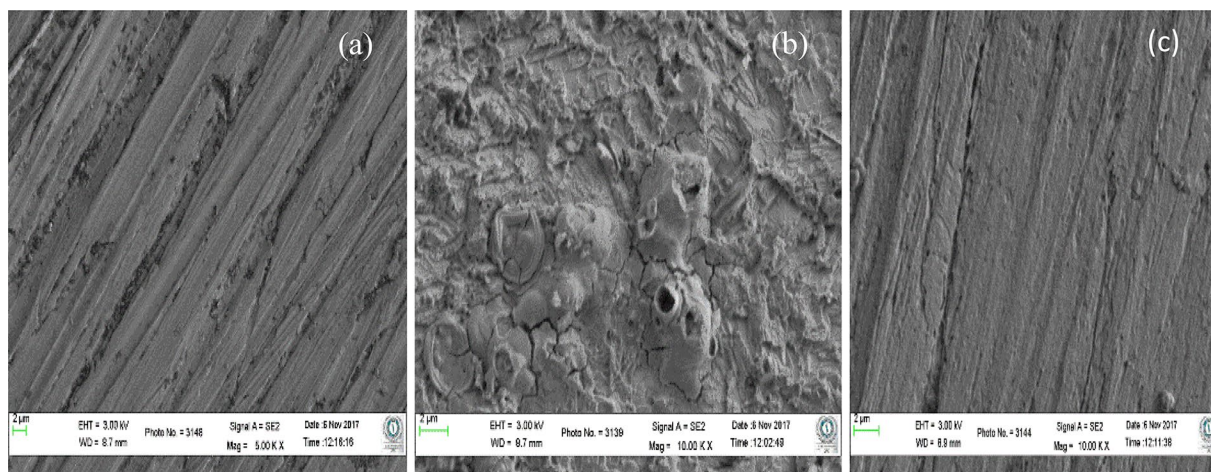


**Fig. 8** SEM images of **a** pure metal, **b** metal in 1 M HCl and **c** metal immersed in 600 ppm inhibitor solution

with the increase in the concentration as more number of active molecules of the inhibitor get adsorbed on the metal surface and also may be due to the formation of  $\text{Fe}^{2+}$  beta carotene complex on the metal surface. The increase in IE % with raise in temperature upto 333 K suggests chemical interaction between the inhibitor molecules and the metal surface. This is further supported by the  $E_a$  and enthalpy values. Adsorption studies show that it obeyed modified Langmuir isotherm and support the monolayer adsorption. The negative value of  $\Delta G^{\circ}_{\text{ads}}$  indicates the spontaneity of adsorption. The higher value of  $K_{\text{ads}}$  with increase in temperature infers increased adsorption rather than desorption. Potentiodynamic polarisation studies reveal that the inhibition was mixed type inhibiting both the anodic metal dissolution and cathodic hydrogen evolution. The impedance measurements indicated that there was an increase both in the surface coverage of the inhibitor and the thickness of the electrical double layer reflecting the efficiency of the inhibitor. The UV–Vis, FTIR spectral studies and surface analytical study using SEM agree to the formation of the protective layer on the metal surface.

**Acknowledgements** One of the authors S.J. Hepziba wishes to thank Centre for Research, CHRIST (Deemed to be University) for providing the financial support and Ms. Jilna Jomy I MSc chemistry for her involvement in carrying out a part of the research work.

### Compliance with Ethical Standards

**Conflict of interest** The authors declare that they have no conflict of interest.

### References

- Li LF, Caenen P, Celis JP (2008) Effect of hydrochloric acid on pickling of hot-rolled 304 stainless steel in iron chloride-based electrolytes. *Corros Sci* 50:804–810. <https://doi.org/10.1016/j.corsci.2007.09.006>
- Ken Dibble GS, Wansbrough, H (2003) Chemical cleaning of metals. VIII-Metals-H-Cleaning-2, NZ Inst. Chem., pp 1–9
- Raja PB, Ismail M, Ghoreishiamiri S et al (2016) Reviews on corrosion inhibitors: a short view. *Chem Eng Commun* 203:1145–1156. <https://doi.org/10.1080/00986445.2016.1172485>
- Krishnaveni K, Ravichandran J (2014) Effect of aqueous extract of leaves of *Morinda tinctoria* on corrosion inhibition of aluminium surface in HCl medium. *Oral Oncol* 50:2704–2712. [https://doi.org/10.1016/S1003-6326\(14\)63401-4](https://doi.org/10.1016/S1003-6326(14)63401-4)
- Al-Otaibi MS, Al-Mayouf AM, Khan M et al (2014) Corrosion inhibitory action of some plant extracts on the corrosion of mild steel in acidic media. *Arab J Chem* 7:340–346. <https://doi.org/10.1016/j.arabj.2012.01.015>
- Yuli Y, Emriadi, Novesar J, Gunawarman (2015) *Asian Journal of Chemistry*. *Asian J Chem* 27:875–881
- Zuo R (2007) Biofilms: Strategies for metal corrosion inhibition employing microorganisms. *Appl Microbiol Biotechnol* 76:1245–1253. <https://doi.org/10.1007/s00253-007-1130-6>
- Priyadarshani I, Rath B (2012) Commercial and industrial applications of micro algae—a review. *J Algal Biomass Util* 3:89–100
- Wolkers H, Barbosa MJ, Kleinegris DMM, Bosma R, Wijffels RH (2011) Microalgae: the green gold of the future?: large-scale sustainable cultivation of microalgae for the production of bulk commodities. *UR-Food & Biobased Research*, Wageningen, p 32
- Colla LM, Oliveira Reinehr C, Reichert C, Costa JAV (2007) Production of biomass and nutraceutical compounds by *Spirulina platensis* under different temperature and nitrogen regimes. *Bioresour Technol* 98:1489–1493. <https://doi.org/10.1016/j.biortech.2005.09.030>
- Sajilata MG, Singhal RS, Kamat MY (2008) Fractionation of lipids and purification of  $\gamma$ -linolenic acid (GLA) from *Spirulina platensis*. *Food Chem* 109:580–586. <https://doi.org/10.1016/j.foodchem.2008.01.005>
- Madhyastha HK, Vatsala TM (2007) Pigment production in *Spirulina fusciformis* in different photophysical conditions. *Biomol Eng* 24:301–305. <https://doi.org/10.1016/j.bioeng.2007.04.001>
- Machu L, Misurcova L, Ambrozova JV et al (2015) Phenolic content and antioxidant capacity in algal food products. *Molecules* 20:1118–1133. <https://doi.org/10.3390/molecules20011118>



14. Piñero Estrada J (2001) Antioxidant activity of different fractions of *Spirulina platensis* protean extract. *Farm* 56:497–500. [https://doi.org/10.1016/S0014-827X\(01\)01084-9](https://doi.org/10.1016/S0014-827X(01)01084-9)
15. Rajendran S, Paulraj JR (2017) Corrosion behaviour of metals in artificial saliva in presence of spirulina powder. *African J Dent* 5:063–070
16. Sribharathy V, Rajendran S (2012) Corrosion inhibition by green inhibitor : sodium metavanadate –spirulina system correspondence. *Chem Sci Rev Lett* 1:25–29
17. Kamal C, Sethuraman MG (2012) *Spirulina platensis*—a novel green inhibitor for acid corrosion of mild steel. *Arab J Chem* 5:155–161. <https://doi.org/10.1016/j.arabjc.2010.08.006>
18. Xhanari K, Finšgar M, Knez Hrnčič M et al (2017) Green corrosion inhibitors for aluminium and its alloys: a review. *RSC Adv* 7:27299–27330. <https://doi.org/10.1039/C7RA03944A>
19. Badawy WA, El-rabiei MM (2014) The use of beta-carotene as environmentally safe inhibitor for Cu- Al-Ni alloys corrosion in sulfide polluted chloride solutions. *Chem Mater Res* 6:107–115
20. Sanat Products Ltd. <https://www.sanat.co.in/health-care-products/1/sunova-spirulina-capsules>
21. McCafferty E (2005) Validation of corrosion rates measured by the Tafel extrapolation method. *Corros Sci* 47:3202–3215. <https://doi.org/10.1016/j.corsci.2005.05.046>
22. Palumbo G, Berent K, Proniewicz E, Banaś J (2019) Guar gum as an eco-friendly corrosion inhibitor for pure aluminium in 1-M HCl solution. *Materials (Basel)* 12:2620. <https://doi.org/10.3390/ma12162620>
23. Raghavendra N (2019) Use of expired naftifine drug as corrosion inhibitor for copper in hydrochloric acid. *J Adv Electrochem* 5:177–179
24. Rugmini Ammal P, Prajila M, Joseph A (2018) Effective inhibition of mild steel corrosion in hydrochloric acid using EBI-MOT, a 1, 3, 4-oxadiazole derivative bearing a 2-ethylbenzimidazole moiety: electro analytical, computational and kinetic studies. *Egypt J Pet* 27:823–833. <https://doi.org/10.1016/j.ejpe.2017.12.004>
25. Athar M, Ali H, Quraishi MA, Quraishi MA (2016) Corrosion inhibition of carbon steel in hydrochloric acid by organic compounds containing heteroatoms. *Br Corros J* 0599:1–5. <https://doi.org/10.1179/000705902225002376>
26. Huang DQ, Duong T, Nam PC (2019) Effect of the Structure and Temperature on Corrosion Inhibition of Thiourea Derivatives in 1.0 M HCl Solution. *ACS Omega*. <https://doi.org/10.1021/acsomega.9b01599>
27. Menaka R, Subhashini S (2016) Chitosan schiff base as eco-friendly inhibitor for mild steel corrosion in 1 M HCl. *J Adhes Sci Technol* 30:1622–1640. <https://doi.org/10.1080/01694243.2016.1156382>
28. Alhaffar MT, Umoren SA, Obot IB, Ali SA (2018) Isoxazolidine derivatives as corrosion inhibitors for low carbon steel in HCl solution: experimental, theoretical and effect of KI studies. *RSC Adv* 8:1764–1777. <https://doi.org/10.1039/c7ra11549k>
29. Sanni O, Popoola API, Fayomi OSI (2019) Temperature effect, activation energies and adsorption studies of waste material as stainless steel corrosion inhibitor in sulphuric acid 0.5 M. *J Bio Tribo Corros* 5:1–8. <https://doi.org/10.1007/s40735-019-0280-2>
30. Riggs OL Jr, Hurd RM (1967) Temperature coefficient of corrosion inhibition. *Corros. NACE* 23:252–258
31. Menaka R, Subhashini S (2017) Chitosan schiff base as effective corrosion inhibitor for mild steel in acid medium. *Polym Int*. <https://doi.org/10.1002/pi.5245>
32. Tang L, Mu G, Liu G (2003) The effect of neutral red on the corrosion inhibition of cold rolled steel in 1.0 M hydrochloric acid. *Corros Sci* 45:2251–2262. [https://doi.org/10.1016/S0010-938X\(03\)00046-5](https://doi.org/10.1016/S0010-938X(03)00046-5)
33. Noor AE (2007) Temperature effects on the corrosion inhibition of mild steel in acidic solutions by aqueous extract of fenugreek leaves. *Int J Electrochem Sci* 2:996–1017
34. Attar T, Larabi L, Harek Y (2014) Inhibition effect of potassium iodide on the corrosion of carbon steel (XC 38) in acidic medium. *Int J Adv Chem* 2:139–142. <https://doi.org/10.14419/ijac.v2i2.3272>
35. Ben Aoun S (2017) On the corrosion inhibition of carbon steel in 1 M HCl with a pyridinium-ionic liquid: chemical, thermodynamic, kinetic and electrochemical studies. *RSC Adv* 7:36688–36696. <https://doi.org/10.1039/c7ra04084a>
36. Chakravarthy MP, Mohana KN (2014) Adsorption and corrosion inhibition characteristics of some nicotinamide derivatives on mild steel in hydrochloric acid solution. *ISRN Corros* 2014:1–13. <https://doi.org/10.1155/2014/687276>
37. Lagren M (2002) Study of the mechanism and inhibiting 4H–1, 2, 4-triazole on mild steel corrosion in acidic media. *Corros Sci* 44:573–588. [https://doi.org/10.1016/S0010-938X\(01\)00075-0](https://doi.org/10.1016/S0010-938X(01)00075-0)
38. Umoren SA, Eduok UM, Solomon MM, Udoh AP (2016) Corrosion inhibition by leaves and stem extracts of *Sida acuta* for mild steel in 1 M H<sub>2</sub>SO<sub>4</sub> solutions investigated by chemical and spectroscopic techniques. *Arab J Chem* 9:S209–S224. <https://doi.org/10.1016/j.arabjc.2011.03.008>
39. Benabdellah M, Tounsi A, Khaled KF, Hammouti B (2011) Thermodynamic, chemical and electrochemical investigations of 2-mercapto benzimidazole as corrosion inhibitor for mild steel in hydrochloric acid solutions. *Arab J Chem* 4:17–24. <https://doi.org/10.1016/j.arabjc.2010.06.010>
40. Sanja Martinez IS (2002) Thermodynamic characterization of metal dissolution and inhibitor adsorption processes in the low carbon steel/mimosa tannin/sulfuric acid system. *Appl Surf Sci* 199:83–89
41. Yaro AS, Khadom AA, Wael RK (2013) Apricot juice as green corrosion inhibitor of mild steel in phosphoric acid. *Alexandria Eng J* 52:129–135. <https://doi.org/10.1016/j.aej.2012.11.001>
42. Arukalam IO, Madu IO, Ijomah NT et al (2014) Acid corrosion inhibition and adsorption behaviour of ethyl hydroxyethyl cellulose on mild steel corrosion. *J Mater* 2014:1–11. <https://doi.org/10.1155/2014/101709>
43. Preethi Kumari P, Shetty P, Rao SA (2017) Electrochemical measurements for the corrosion inhibition of mild steel in 1 M hydrochloric acid by using an aromatic hydrazide derivative. *Arab J Chem* 10:653–663. <https://doi.org/10.1016/j.arabjc.2014.09.005>
44. Li WH, He Q, Zhang ST et al (2008) Some new triazole derivatives as inhibitors for mild steel corrosion in acidic medium. *J Appl Electrochem* 38:289–295. <https://doi.org/10.1007/s10800-007-9437-7>
45. Al-Amiery AA, Kadhum AAH, Kadhim A et al (2014) Inhibition of mild steel corrosion in sulfuric acid solution by new schiff base. *Materials (Basel)* 7:787–804. <https://doi.org/10.3390/ma7020787>
46. Karthikaiselvi R, Subhashini S (2014) Study of adsorption properties and inhibition of mild steel corrosion in hydrochloric acid media by water soluble composite poly (vinyl alcohol-o-methoxy aniline). *J Assoc Arab Univ Basic Appl Sci* 16:74–82. <https://doi.org/10.1016/j.jaubas.2013.06.002>
47. El Aoufir Y, Sebhaoui J, Chaouiki A et al (2018) Two novel benzodiazepines as corrosion inhibitors for carbon steel in hydrochloric acid: experimental and computational studies. *J Bio Tribo Corros*. <https://doi.org/10.1007/s40735-018-0169-5>
48. Singh A, Caihong Y, Yaocheng Y et al (2019) Analyses of new electrochemical techniques to study the behavior of some corrosion mitigating polymers on n80 tubing steel. *ACS Omega* 4:3420–3431. <https://doi.org/10.1021/acsomega.8b02983>
49. Zehra S, Mobin M, Aslam J, Parveen M (2018) Assessment of glycine derivative N-benzylidene-2((2-oxo-2-(10H-phenothiazine-10yl)ethyl)amino) acetohydrazide as inhibitor for mild



- steel corrosion in 1 M HCl solution: electrochemical and theoretical approach. *J Adhes Sci Technol* 32:317–342. <https://doi.org/10.1080/01694243.2017.1354669>
50. Popova A, Raicheva S, Sokolova E, Christov M (1996) Frequency dispersion of the interfacial impedance at mild steel corrosion in acid media in the presence of benzimidazole derivatives. *Langmuir* 12:2083–2089
  51. Acid H, Lgaz H, Masroor S et al (2020) Evaluation of 2-mercapto-benzimidazole derivatives as corrosion inhibitors for mild steel in hydrochloric acid. *Metals (Basel)* 10:1–14
  52. Parveen M, Mobin M, Zehra S, Aslam R (2018) L-proline mixed with sodium benzoate as sustainable inhibitor for mild steel corrosion in 1M HCl: an experimental and theoretical approach. *Sci Rep* 8:1–18. <https://doi.org/10.1038/s41598-018-24143-2>
  53. Xu X, Singh A, Sun Z et al (2017) Theoretical, thermodynamic and electrochemical analysis of biotin drug as an impending corrosion inhibitor for mild steel in 15% hydrochloric acid. *R Soc Open Sci*. <https://doi.org/10.1098/rsos.170933>
  54. Singh P, Ebenso EE, Olasunkanmi LO et al (2016) Electrochemical, theoretical, and surface morphological studies of corrosion inhibition effect of green naphthyridine derivatives on mild steel in hydrochloric acid. *J Phys Chem C* 120:3408–3419. <https://doi.org/10.1021/acs.jpcc.5b11901>
  55. Belarbi Z, Dominguez Olivo JM, Farelas F et al (2019) Decanethiol as a corrosion inhibitor for carbon steels exposed to aqueous CO<sub>2</sub>. *Corrosion* 75:1246–1254. <https://doi.org/10.5006/3233>
  56. Alaneme KK, Olusegun SJ, Adelowo OT (2016) Corrosion inhibition and adsorption mechanism studies of *Hunteria umbellata* seed husk extracts on mild steel immersed in acidic solutions. *Alexandria Eng J* 55:673–681. <https://doi.org/10.1016/j.aej.2015.10.009>
  57. Shah AM, Rahim AA, Hamid SA, Yahya S (2013) PGreen inhibitors for copper corrosion by Mangrove tannin. *Int J Electrochem Sci* 8:2140–2153
  58. Prabakaran M, Kim SH, Sasireka A et al (2017)  $\beta$ -Sitosterol isolated from rice hulls as an efficient corrosion inhibitor for mild steel in acidic environments. *New J Chem* 41:3900–3907. <https://doi.org/10.1039/c6nj03760g>
  59. Abdel-Gaber AM, Abd-El-Nabey BA, Sidahmed IM et al (2006) Inhibitive action of some plant extracts on the corrosion of steel in acidic media. *Corros Sci* 48:2765–2779. <https://doi.org/10.1016/j.corsci.2005.09.017>
  60. Aloysius A, Ramanathan R, Christy A et al (2018) Experimental and theoretical studies on the corrosion inhibition of vitamins—thiamine hydrochloride or biotin in corrosion of mild steel in aqueous chloride environment. *Egypt J Pet* 27:371–381. <https://doi.org/10.1016/j.ejpe.2017.06.003>
  61. Gadow HS, Motawea MM (2017) Investigation of the corrosion inhibition of carbon steel in hydrochloric acid solution by using ginger roots extract. *RSC Adv* 7:24576–24588. <https://doi.org/10.1039/c6ra28636d>
  62. Dotto GL, Vieira MLG, Esquerdo VM, Pinto LAA (2013) Equilibrium and thermodynamics of azo dyes biosorption onto *Spirulina platensis*. *Braz J Chem Eng* 30:13–21. <https://doi.org/10.1590/S0104-66322013000100003>
  63. Kleinegris DMM, van Es MA, Janssen M et al (2010) Carotenoid fluorescence in *Dunaliella salina*. *J Appl Phycol* 22:645–649. <https://doi.org/10.1007/s10811-010-9505-y>

**Publisher's Note** Springer Nature remains neutral with regard to jurisdictional claims in published maps and institutional affiliations.

## Affiliations

S. J. Hepziba Magie Jessima<sup>1</sup> · S. Subhashini<sup>2</sup> · James Arulraj<sup>1</sup>

✉ S. J. Hepziba Magie Jessima  
hepziba.magie@christuniversity.in

S. Subhashini  
subhash.sethu@gmail.com

<sup>2</sup> Department of Chemistry, Avinashilingam Institute for Home Science and Higher Education for Women (Deemed To Be University), Coimbatore, India

<sup>1</sup> Department of Chemistry, CHRIST (Deemed To Be University), Bengaluru, India